


Evaluation of Vascular Reactivity of Maternal Vascular Adaptations of Pregnancy With Quantitative MRI: Pilot Study

Michael C. Langham, PhD,^{1*}  Alessandra S. Caporale, PhD,¹ Felix W. Wehrli, PhD,¹ Samuel Parry, MD,² and Nadav Schwartz, MD²

Background: Abnormal maternal vascular function during pregnancy stemming from systemic endothelial dysfunction (EDF) has a central role in the pathophysiology of preeclampsia (PE).

Purpose: To utilize quantitative MRI to investigate changes in physiological measures of vascular reactivity during normal pregnancy, and to explore EDF associated with preeclampsia.

Study Type: Prospective.

Population: Healthy pregnant (HP) ($n = 14$, mean GA = 26 ± 7 weeks) and nonpregnant women (NP; $n = 14$); newly postpartum (PP < 48 hours) women with severe PE (PP-PE; $n = 4$) and normotensive pregnancy (PP-HP; $n = 5$).

Field Strength/Sequence: 1.5T/3T. RF spoiled multiecho gradient-recalled echo, 1D phase-contrast MRI, time-of-flight.

Assessment: The micro- and macrovascular function (vasodilatory capacity of arterioles and conduit arteries, respectively) of the femoral vascular bed was evaluated with MRI-based venous oximetry, arterial velocimetry, and luminal flow-mediated dilation quantification, during cuff-induced reactive hyperemia. Aortic arch pulse-wave velocity (aPWV) was quantified to assess arterial stiffness using an ungated 1D technique.

Statistical Tests: Two-tailed unpaired t-tests were performed to address our two, primary a priori comparisons, HP vs. NP, and PP-PE vs. PP-HP. Given the pilot nature of this study, adjustments for multiple comparisons were not performed.

Results: In HP, microvascular function was attenuated compared to NP by a significant increase in the washout time (10 ± 2 vs. 8 ± 2 sec; $P < 0.05$) and reduced upslope (2.1 ± 0.5 vs. $3.2 \pm 0.8\% \text{HbO}_2/\text{s}$; $P < 0.05$), time of forward flow (28 ± 5 vs. 33 ± 6 sec, $P < 0.05$), and hyperemic index (11 ± 3 vs. $16 \pm 4 \text{ cm/s}^2$; $P < 0.05$), but luminal flow-mediated dilation (FMD_l) was comparable between HP and NP. PP-PE exhibited significant vascular dysfunction compared to PP-HP, as evidenced by differences in upslope (2.2 ± 0.6 vs. $1.3 \pm 0.2\% \text{HbO}_2/\text{s}$, $P < 0.05$), overshoot (16 ± 5 vs. $7 \pm 3\% \text{HbO}_2$, $P < 0.05$), time of forward flow (28 ± 6 vs. 15 ± 7 s, $P < 0.05$), and aPWV (7 ± 1 vs. 8 ± 1 m/s, $P < 0.05$).

Data Conclusion: Attenuated vascular reactivity during pregnancy suggests that the systemic vasodilatory state partially depletes nitric oxide bioavailability. Preliminary data support the potential for MRI to identify vascular dysfunction in vivo that underlies PE.

Level of Evidence: 2

Technical Efficacy Stage: 1

J. MAGN. RESON. IMAGING 2021;53:447–455.

PREGNANCY CAN BE CONSIDERED a prolonged “stress test,” given the significant and sustained vascular and hemodynamics changes that occur.¹ Maternal cardiac output increases by 40 to 50%, as a result of profound increases in both plasma volume and heart rate.¹ By mid-

gestation, maternal physiology reaches its most vasodilated state, manifesting as the lowest blood pressure and peripheral vascular resistance for the pregnancy.¹ However, as the plasma volume and cardiac output plateau in the mid-third trimester, maternal blood pressure often surpasses baseline

View this article online at wileyonlinelibrary.com. DOI: 10.1002/jmri.27342

Received May 26, 2020, Accepted for publication Aug 7, 2020.

*Address reprint requests to: M.C.L., Department of Radiology, University of Pennsylvania Health System, 1 Founders Building (MRI Education Center), 3400 Spruce Street, Philadelphia, PA 19104. E-mail: langhamc@penmedicine.upenn.edu

Contract grant sponsor: National Institutes of Health; Contract grant numbers: NIH R01 HL139358, NIH UL1 TR001878, NIH U01 HD087180.

From the ¹Department of Radiology, University of Pennsylvania School of Medicine, Philadelphia, Pennsylvania, USA; and ²Division of Maternal-Fetal Medicine, Department of Obstetrics and Gynecology, University of Pennsylvania School of Medicine, Philadelphia, Pennsylvania, USA

levels.¹ These profound cardiovascular changes are important adaptations that characterize a normal pregnancy.¹

Preeclampsia (PE), one of the greatest contributors to perinatal morbidity and mortality worldwide, affecting 2–8% of all pregnancies, is largely believed to be caused by an underlying maternal endothelial dysfunction (EDF).² In its severe form, PE can manifest with life-threatening events to the mother such as acute renal failure, cerebral edema, stroke, and cardiac failure.³ In addition, PE is a strong independent risk factor for future vascular disease and premature death in women who developed PE during pregnancy.⁴ Therefore, robust and accurate characterization of endothelial function throughout pregnancy could allow for greater understanding of the underlying normal and pathologic EDF. Further, to help close the significant gaps in understanding and detecting the underlying pathophysiology of this disease and its association with future cardiovascular events.⁵

Ultrasound (US) measurements of flow-mediated dilatation (FMD) in the brachial artery following cuff-induced ischemia is currently the research standard for noninvasive assessment of endothelial function.⁶ During reactive hyperemia, the increased shear rate on the endothelium leads to vasodilation of the conduit artery via nitric oxide (NO) release.⁷ While often regarded as an effective surrogate marker for endothelial function, brachial artery FMD is limited by poor intrasubject reproducibility, with the coefficients of variation of FMD measurements varying widely from as little as 1.5% to ~50% in others.^{8–10} This limitation is magnified, since the average magnitude of FMD is ~5% and US settings such as dynamic range, gain, and probe distance are known to significantly affect diameter measurements.^{11,12} Consequently, poor reproducibility and standardization have contributed to conflicting FMD data in the pregnant population, including those who developed PE.^{13,14}

Arterial tonometry is another cardiovascular research tool that is utilized to estimate pulse-wave velocity (PWV), a physiologic marker of arterial stiffness that has been used to study the vascular effects of aging, cardiovascular disease, stroke, renal dysfunction, cognitive disorders, and smoking.^{15–18} Tonometry measures the time delay of the systolic pressure wave at some downstream location using pressure transducers placed at the two locations (typically the common carotid and femoral arteries).¹⁹ However, tonometry has several significant limitations, which include imprecise estimation of the path length of the pressure wave, difficulty in obtaining the femoral pressure waveform, and inability to target regional PWV measurement of the aortic arch, which is the main elastic reservoir of the cardiovascular system mainly responsible for the pathophysiological effects of arterial stiffening due to its proximity to the left ventricle.^{20,21} These limitations have led some experts to be cautious of the validity and reproducibility of this technique in the evaluation of vascular function.²⁰ Nonetheless, significant associations between carotid-femoral PWV

and PE have been reported and may even persist for some time after delivery.^{22,23}

In this study we present an innovative quantitative magnetic resonance imaging (MRI) protocol for assessing normal and pathologic vascular reactivity in pregnancy. These MRI techniques have demonstrated their value and detection sensitivity in the study of various pathologic states and physiologic challenges, including peripheral artery disease and chronic exposure to cigarette smoking, as well as the acute effects of electronic cigarette aerosol inhalation.^{24–26} The objective of this pilot study was to demonstrate the feasibility and potential utility of these MRI techniques in studying pregnancy-related vascular pathophysiology.

Materials and Methods

Participants

VASCULAR REACTIVITY IN HEALTHY PREGNANT (HP) VS. HEALTHY NONPREGNANT (NP). In pregnant subjects, multiple gestation and known fetal anomalies were excluded from participation. The pregnancy status was monitored under prenatal care per clinical routine and collection of outcomes. Data for nonpregnant, healthy controls were retrieved from a database of a recent study that some of the present authors had completed using the same MRI techniques.²⁶

VASCULAR REACTIVITY IN POSTPARTUM SEVERE PE VS. POSTPARTUM NORMOTENSIVE. Postpartum (PP) PE subjects were diagnosed and treated for severe PE by their clinical team during term delivery and then approached for participation after delivery. At our institution, severe PE is defined based on current American College of Gynecology guidelines, most commonly with newly elevated blood pressures >160/110 mmHg and one of the following: headache, visual disturbances, or signs of end-organ damage such as proteinuria, renal insufficiency, elevated liver function test, thrombocytopenia, or pulmonary edema.²⁷ Subjects were approached for participation after delivery and MRI exams were performed between 24 and 48 hours after delivery. Normotensive PP controls with similar age (± 5 years), race, body mass index (BMI) (± 5 kg/m²), and gestational age (± 1 week) were recruited.

All subjects were recruited with written informed consent obtained prior to all examinations following an Institutional Review Board-approved protocol. Subjects were between 18 and 35 years of age, with BMI ≤ 35 , and no history of cardiovascular disease, diabetes, or connective tissue disorders.

Quantitative MRI Protocol

All MRI on pregnant and postpartum women were performed with a clinical 1.5T Siemens Avanto (Siemens Medical Solutions, Erlangen, Germany) unit, using standard RF coils (a circularly polarized extremity coil for imaging the femoral vessels, a body matrix combined with spine coil for aortic arch). The entire protocol, including scout scans, lasted less than 40 minutes and the patients were scanned in feet-first supine position for the cuff-occlusion paradigm (25 minutes, including patient setup and localizer scans) and head-first supine for aortic PWV quantification (15 minutes, with

10 minutes for patient repositioning and localizer scans). Subjects were given a 5-minute break between each scanning position.

The data for the healthy nonpregnant women were obtained from the control group of a recent study performed by some of the authors exploring the acute effects of e-cigarette smoke inhalation. In that study, the MRI protocol was structurally identical and acquired the same set of physiological parameters, although using a clinical 3T Siemens Prisma (Siemens Medical Solutions).²⁶ For the healthy pregnant and nonpregnant groups, the MRI protocol was expanded to also include the quantification of femoral artery luminal FMD (FMD_L).

ASSESSMENT OF PERIPHERAL MICRO- AND MACROVASCULAR ENDOTHELIAL FUNCTION.

Briefly, lower limb ischemia was induced by applying a blood pressure cuff (SC120D model, Hokanson, Bellevue, WA) to the upper right thigh, on the adductor longus region. The cuff was inflated to 100 mmHg above the subject's systolic blood pressure (SBP), but not exceeding 250 mmHg to occlude the superficial femoral artery (SFA) and vein (SFV). The MRI examination during cuff paradigm consisted of 2 minutes of baseline imaging, 5 minutes of cuff occlusion, and 5 minutes of imaging during recovery (reactive hyperemia). During the baseline (preocclusion) period, SFA blood flow velocity, lumen area, and SFV oxygenation (SvO₂) were quantified successively. During reactive hyperemia (postocclusion), blood flow velocity and oxygenation level were simultaneously time-resolved with a temporal resolution of 150 msec and 2 seconds, respectively, but suspended at 60, 90, 120, 180, and 240 seconds after cuff deflation to acquire high-spatial resolution time-of-flight (0.625 mm) images to estimate the maximum SFA FMD_L. Quantification of SvO₂ was performed with MR susceptometry-based oximetry, a field-mapping method, where images were acquired with a multiecho RF-spoiled gradient-recalled echo (GRE) sequence.²⁸ Absolute blood flow velocity waveform was time-resolved without gating via a 1D version of phase-contrast (PC)-MRI.²⁹

ASSESSMENT OF AORTIC ARCH STIFFNESS. Aortic arch pulse-wave velocity (aPWV) was quantified by estimating the propagation time of the velocity wave from ascending aorta to proximal descending aorta. The foot and the systolic wave front of velocity wave was time-resolved by sampling velocity-encoded center *k*-space line *k_y* = 0 repeatedly without gating.³⁰

The pulse sequences used and their acquisition parameters are summarized in Table 1. The MRI metrics that parameterize the time-courses of SvO₂ and blood flow velocity are also included in the table along with their physiological interpretations.

Image and Data Analysis

All image reconstruction and image-based quantification of MRI parameters were performed offline by the first author (10+ years of experience).

The field maps or phase difference images $\Delta\phi_{\text{map}}$ for SvO₂ quantification was constructed as $\Delta\phi_{\text{map}} = \arg(Z_2, Z_1^*)$ where *Z*₁ and *Z*₂ represent complex images of first and second echo, respectively, and the asterisk denotes complex conjugate. The effect of low spatial-frequency modulations of the phase caused by large-scale induced magnetic fields was reduced by fitting, after appropriate

weighting and masking, the static field inhomogeneity to a second-order polynomial.³¹ The venous oxygen saturation, SvO₂, in the femoral vein was computed as $100 \times \left(1 - \frac{6\Delta\phi/\Delta TE}{\gamma\Delta\chi_{\text{do}}\text{Hct}\cdot B_0(3\cos^2\theta - 1)}\right)$, where $\Delta\phi$ is the average intravascular femoral vein phase relative to average intravascular femoral artery phase (assumed 100% oxygenation level), ΔTE is the echo spacing, γ is the gyromagnetic ratio of water protons, $\Delta\chi_{\text{do}} = 4\pi \times (0.27 \pm 0.02)$ ppm is the susceptibility difference between fully deoxygenated and fully oxygenated erythrocytes in SI units, θ is the vessel tilt angle relative to the main field *B*₀, and Hct (hematocrit) is the volume fraction of erythrocytes in packed blood.²⁴ The intravascular phase of was measured as the average in a region of interest (ROI) placed at the center of the cross-sectional area of the vessel.

The high-resolution bright-blood images were binarized using automated thresholding based on the entropy method.³² Luminal FMD (FMD_L) was computed as $\frac{(A - A_0)}{A_0} \times 100$. To a first-order approximation, FMD_L doubles the sensitivity of conventional ultrasound-based FMD that relies on the change in diameter, ie, $FMD_L \equiv \delta A/A_0 \approx 2\delta r/r_0$, where δr and *r*₀ are the changes in radius, and radius of the artery at rest, respectively.

In 1D PC-MRI, the phase difference between velocity-encoded projections was computed after removing the interfering background tissue signal. The signal from flowing blood was isolated by masking out the vessels of interest from a reference image (fully sampled *k*-space). The masked image was then Fourier-transformed back to *k*-space. The resulting projection obtained from the center *k*-space line (containing background tissue signal only) was subtracted from the velocity-encoded projections prior to computing the phase difference $\Delta\phi_{\text{vel}}$ and converted to velocity image, $\pi\Delta\phi_{\text{vel}}/\text{VENC}$; VENC is the user-defined velocity sensitivity parameter representing the velocity value that will lead to flow-induced phase accumulation of $\pm\pi$. Spatially averaged velocities of the vessels of interest were computed by averaging the velocity along the readout direction within the vessel boundaries.

Aortic PWV was determined as *L*/ Δt , where *L* and Δt are the path length and transit time of the velocity wave, respectively, from ascending to proximal descending aorta. *L* was manually determined from a sagittal oblique image of the aorta and Δt was determined via the "foot-to-foot" method, routinely performed in tonometry, from the jointly plotted time course of complex difference signal intensity |CD| in ascending and descending aorta.²⁰ The complex difference signal intensity |CD| retains only the signal from the moving spins and represents average signal across the lumen in the projection direction (perpendicular to the readout direction).

All analyses, except FMD_L, required manually drawing an ROI, but within vessel lumen, which considerably reduced subjectivity. A recent reproducibility study performed in 10 participants resulted in intraclass correlation coefficients (ICCs) greater than 0.9 for oximetric parameters and aortic PWV. The hemodynamic parameters achieved ICC >0.8.²⁶

Statistical Analysis

Descriptive analyses were performed for each of the four groups of subjects: 1) healthy pregnant (HP); 2) healthy nonpregnant (NP); 3) postpartum preeclamptic pregnancy (PP-PE); and 4) postpartum healthy pregnancy (PP-HP). Then two-tailed unpaired *t*-tests were

TABLE 1. Pulse Sequence and Imaging Acquisition Parameters

Purpose	Pulse sequence	Acquisition parameters	MRI metrics	Interpretation
Peripheral vascular bed				
MR susceptometry (SFV)	RF-spoiled multiecho GRE	TE/TR = 5/50 ms, flip angle = 18°, echo spacing = 8.24 ms FOV = 160 mm, slice thickness = 5 mm, matrix = 160 × 40 (keyhole acquisition scheme), BW = 250 Hz/pix	Washout (s) Upslope (%HbO ₂ /s) Overshoot (%HbO ₂)	Draining time of tagged capillary blood. Tissue re-saturation rate. Degree of over compensation of tissue oxygenation.
1D PC-MRI (SFA)	RF-spoiled GRE	TE/TR = 5.2/10 ms, flip angle = 15°, VENC = 80 cm/s (baseline)	Hyperemic index, HI (cm/s ²) Peripheral flow reserve, PFR	Initial acceleration of transient hyperemia. Avg peak-to-avg baseline velocity.
TOF (SFA)	RF-spoiled GRE	TE/TR = 5.5/50 ms, flip angle = 18°, VENC = 175 cm/s (postocclusion)	Forward flow time, T _{FF} (s)	Duration of reduced microvascular resistance.
Aortic arch			Femoral artery FMD _L (%)	Maximum increase in luminal area during reactive hyperemia.
1D PC-MRI (aorta)	RF-spoiled GRE	TE/TR = 5.8/34.72 ms, flip angle = 20° TE/TR = 2.1/3.7 ms, flip angle = 15°, VENC = 300 cm/s	Femoral artery FMD _L (%) Pulse-wave velocity, PWV (m/s)	Maximum increase in luminal area during reactive hyperemia. Central artery stiffness

SFV = superficial femoral vein; SFA = superficial femoral artery; RF = radiofrequency; GRE = gradient-recalled echo; BW = bandwidth.

performed to address our two, primary a priori comparisons, HP vs. NP and PP-PE vs. PP-HP, with $P < 0.05$ considered significant.

Results

The profiles of study subjects are summarized in Table 2. A total of 14 healthy pregnant women ($n = 14$, mean gestational age, 26.4 ± 6.5) and 14 nonpregnant controls were included. Preeclampsia did not ensue in pregnant women. In addition, nine postpartum subjects (four with severe PE) were also examined. The total recruitment number for postpartum women with severe PE pregnancy was 7. Three withdrew and the reasons included change of mind before entering the scanner, claustrophobia, and failure of cuff occlusion.

Representative time-courses of SvO₂ and blood flow velocity during reactive hyperemia of a healthy pregnant and nonpregnant women are jointly shown in Fig. 1. For the velocity time-course, only the sliding window average for the healthy nonpregnant is shown for clarity. In Fig. 2 sample high-resolution bright-blood and binarized images are shown.

In Fig. 3a the oblique sagittal localizer image of aorta shows the location of the imaging plane that enables simultaneous quantification of velocity-encoded projections at proximal ascending and descending aorta (Fig. 3a,b). The axial reference image (Fig. 3c) helps identify ascending and descending aorta on the time-resolved |CD| image of Fig. 3d.

In pregnant subjects micro- and macrovascular function was attenuated compared to nonpregnant women (Fig. 4). There was a significant increase in the washout time (10 ± 2 vs. 8 ± 2 sec; $P < 0.05$) and reduction in both the upslope (2.1 ± 0.5 vs. $3.2 \pm 0.8\% \text{HbO}_2/\text{s}$; $P < 0.05$), T_{FF} (28 ± 5 vs. 33 ± 6 sec; $P < 0.05$), and hyperemic index (HI) (11 ± 3 vs. $16 \pm 4 \text{ cm/s}^2$; $P < 0.05$) between pregnant vs. nonpregnant subjects. The observed differences in aortic arch PWV (7 ± 1 vs. 6 ± 1 m/s; $P = 0.081$) and superficial femoral artery FMD_L (20 ± 10 vs. $13 \pm 3\%$; $P = 0.357$) between the pregnant and nonpregnant women were not significantly different in this small, pilot study.

Impaired vascular function was observed when comparing MRI parameters between the postpartum women with

and without severe PE (Fig. 5). Most notably, in the former there were significant reductions in upslope (1.3 ± 0.6 vs. $2.2 \pm 0.6\% \text{HbO}_2/\text{s}$, $P < 0.05$), overshoot (7 ± 3 vs. $16 \pm 5\% \text{HbO}_2$, $P < 0.05$), and T_{FF} (15 ± 6 vs. 28 ± 6 s, $P = 0.037$). In addition, the regional PWV in the aortic arch was also elevated (8 ± 1 vs. 7 ± 1 m/s, $P < 0.05$) in women who had preeclamptic pregnancy compared to those who had a normal pregnancy.

Discussion

In this pilot study, the primary objective was to present a non-invasive quantitative MRI protocol for evaluating endothelial function as a potential new imaging tool to help understand the unique vascular reactivity of healthy, pregnant women carrying nonanomalous, singleton gestations. Further, in order to study the pathophysiology of preeclampsia, we recruited newly postpartum women who were diagnosed and treated for severe PE by their clinical team during term delivery. We elected to focus on the postpartum period since pregnant women with severe PE at term require hospital admission and delivery, making delaying their care for a research MRI inappropriate. In addition, as the pathophysiology of severe PE remains active to a large degree for days to weeks after delivery, this would still allow us to preliminarily test our quantitative MRI techniques in the study of this disease process. The preliminary MRI data indicate that a significant attenuation in vascular function is present in pregnant compared to nonpregnant women. Although the preliminary data indicate that this MRI strategy detects differences in vascular function in newly postpartum women with severe PE compared to postpartum normotensive controls, it should be interpreted with caution due to the limited sample size. However, the results highlight the potential for this MRI approach to enable quantitative, in vivo investigations of vascular function in pregnancy.

MRI oximetric parameters are more recently developed measures of microvascular function and add an entirely new functional dimension to the evaluation of vascular function compared to brachial artery FMD and carotid-femoral PWV.²⁴ During cuff occlusion, arterial supply is suspended,

TABLE 2. Subject Profile

Parameter	Pregnant $n = 14$	Nonpregnant $n = 14$	Postpartum (normal) $n = 5$	Postpartum (PE) $n = 4$
Maternal age, year	24.8 ± 6.2	23.7 ± 3.9	31.1 ± 6.5	29.3 ± 3.1
Ethnic group				
White	4	11	0	0
Black	9	2	5	4
Other	1	1	0	0
BMI, kg/m ²	26.3 ± 4.3	22.1 ± 2.2	25.5 ± 4.9	25.5 ± 4.0

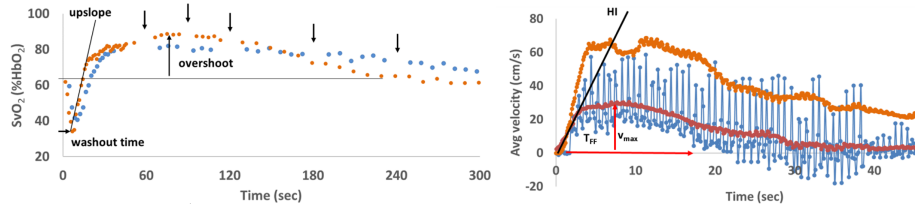


FIGURE 1: Parameterization of dynamic oximetry and velocimetry time-course for quantifying reactive hyperemia. (a) Time-courses of capillary blood oxygen saturation quantified at the superficial femoral vein of a pregnant (blue) and nonpregnant (orange) women. Cuff release occurs at $t = 0$. Black arrows indicate suspension of dynamic oximetry for high-resolution imaging to estimate femoral artery FMD. (b) Pregnant woman arterial blood flow velocity time-course (blue) showing individual systolic peaks with red and orange lines representing 3-second sliding-window average of pregnant and nonpregnant women, respectively. V_{max} divided by the baseline average velocity (not shown) is related to the peripheral flow reserve (PFR). See text for definitions of parameters.

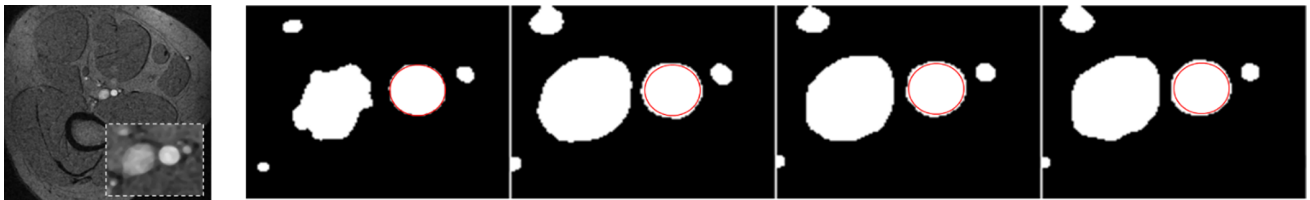


FIGURE 2: Femoral artery luminal FMD. (a) Sample high-resolution bright-blood magnitude image. Inset shows a magnified view of superficial femoral vessels. (b) Binarized images for quantifying luminal area. The first image was acquired prior to cuff occlusion and for demonstration purposes; subsequent images correspond to 60, 90, and 120 seconds after the cuff deflation. Red circle is overlaid to facilitate visualization of dilation relative to baseline (first image). In this pregnant subject the maximum luminal FMD was 18%, corresponding to a 9% increase in vessel diameter occurring at 60 seconds after cuff deflation.

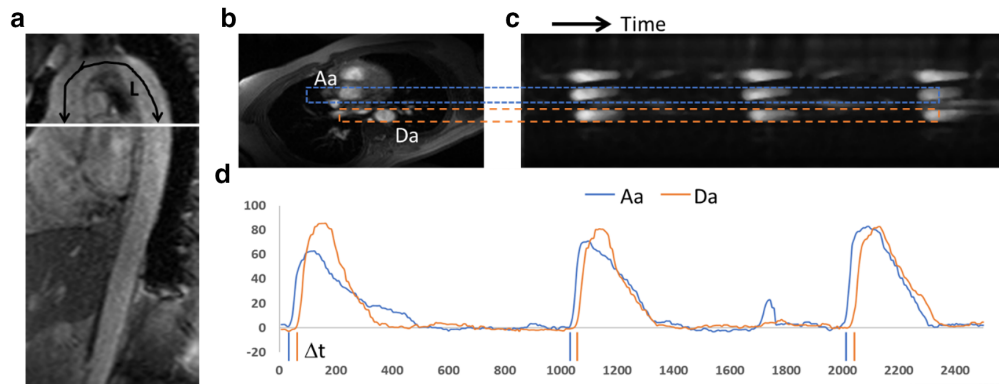


FIGURE 3: Noncardiac triggered aortic PWV quantification. (a) Oblique sagittal image of the aorta for velocity wave path length L (black line) estimation. The white line indicates the prescribed slice position of the (b) reference axial image. It is rotated (readout direction is vertical) to enable identification of the ascending (Aa) and descending aorta (Da) on the velocity-dependent intensity image of (c) as denoted by the dashed rectangles. Three systolic peaks are shown. (d) Time-course of signal intensity generated from (c) clearly showing transit delay Δt of the velocity wave at Da relative to Aa. PWV was computed as $L/\Delta t$.

but oxygen extraction continues in the capillary bed. Therefore, the partially desaturated blood in the microvascular capillary bed serves as an endogenous tracer. Upon cuff deflation, rapid replacement of desaturated capillary blood by normally oxygenated venous blood is monitored in the draining superficial femoral vein with MR oximetry and the time-course of SvO_2 . Washout time estimates how quickly the tagged blood in the capillary bed is “flushed” out of the tissue, hence reflecting microvascular reactivity.³³ Similarly, rapid drainage, signifying healthy endothelial function in the microvasculature,²⁴ manifests as a higher rate of resaturation (upslope) and the degree of supply exceeding the demand is characterized by greater overshoot.

In a previous study, comparisons between young healthy nonsmokers and young smokers, oximetric parameters were shown to be more predictive in detecting the deleterious effects of aging and smoking on endothelial function compared to brachial artery FMD. A significant difference was observed in the washout time and upslope was observed among young smokers.²⁵ In this study, both washout time and upslope parameters were also significantly different in pregnant women compared to nonpregnant controls. Among postpartum women, upslope and overshoot were significantly lower in those who had preeclamptic pregnancy. These preliminary results, albeit encouraging, are based on a limited sample size; therefore, further study is warranted to interpret

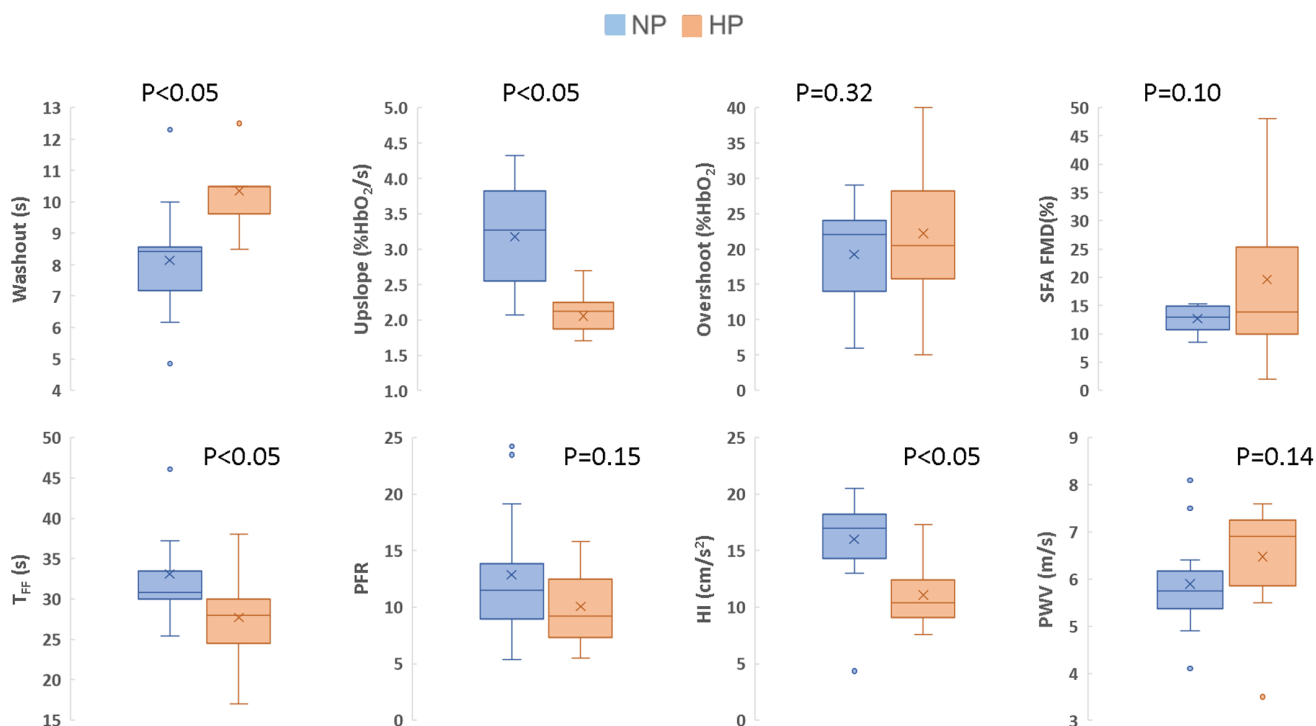


FIGURE 4: MRI surrogate markers of EDF quantified in healthy nonpregnant (NP) and healthy pregnant (HP) women. Significantly prolonged washout time and decreased upslope, T_{FF} , and HI in pregnant women compared to nonpregnant controls characterize blunted micro- and macrovascular reactivity. Significant differences in oximetric parameters suggest slower replacement of capillary blood while the hemodynamic parameters suggest reduced bioavailability of NO resulting in attenuated hyperemia. *P* values were derived on the basis of paired *t*-tests. The boxes represent inner quartiles; horizontal lines within the box indicate the median, and crosses (X) indicate the mean.

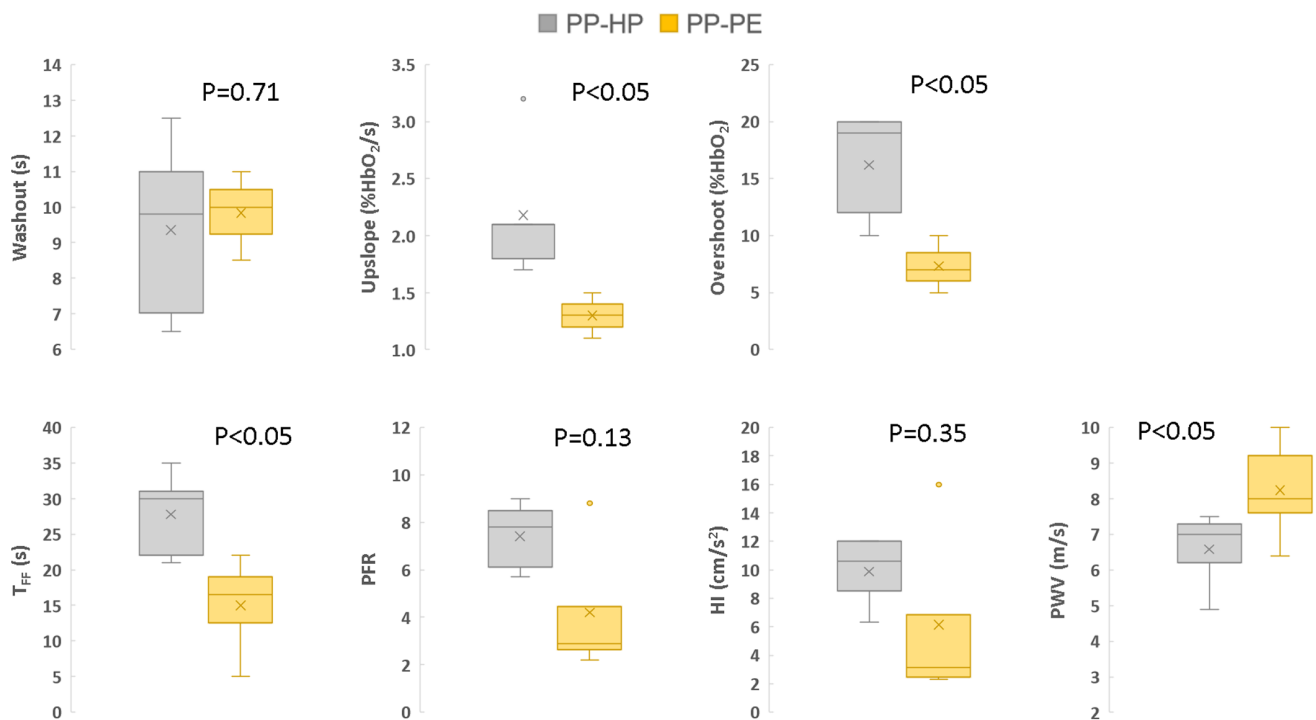


FIGURE 5: Negative impact on MRI surrogate markers of EDF after severe PE pregnancy (PP-PE) relative to healthy pregnancy (PP-HP). Reduced upslope and overshoot indicated slower replacement of desaturated tissue blood by normally oxygenated venous blood. Shorter T_{FF} corresponds to inability achieve reduced microvascular resistance to accommodate hyperemia to full magnitude, resulting in lower PFR.

the results with regard to MRI metrics' potential to provide new insight into microvascular function in preeclamptic pregnancy.

The MRI velocimetric parameters of arterial hemodynamics exhibited differences in vascular function during hyperemia in nonpregnant women in terms of higher initial acceleration of blood flow velocity after cuff deflation (hyperemic index, HI) and longer duration of reduced microvascular resistance (T_{FF}) compared to pregnant women. These results may indicate that the systemic vasodilatory state of pregnancy partially depletes the recruitable endothelial reservoir. In other words, while the reduced systemic vascular resistance may be an essential adaptation in pregnancy to accommodate the significant increases in plasma volume, cardiac output, and uteroplacental perfusion, there are limits to the body's ability to adapt. Consequently, there is an attenuated hyperemic response in pregnancy. In the postpartum PE group, only T_{FF} among hemodynamic parameters was altered compared to normotensive controls, reaching statistical significance. The reduced duration of monophasic velocity profile during hyperemia also suggest a limited bioavailability of nitric oxide.

The MRI approach used in this study also allows for PWV assessment of the aortic arch. Tonometry-based assessments of aortic stiffness in pregnancy have most often targeted carotid-femoral (cf) PWV, with significantly increased cf-PWV being reported in women with PE relative to normotensive pregnancy.^{22,23} Studies have only shown small (<10%) changes in cf-PWV in pregnant compared to nonpregnant women.^{34,35} We did not observe a difference in aortic PWV between healthy pregnant and nonpregnant women but markedly increased arterial stiffness in postpartum subjects with severe PE compared to normotensive controls. During pregnancy, systemic vascular resistance reaches a minimum in the second trimester. This adaptation delays and attenuates peripheral wave reflections and reduces aortic stiffness.^{20,36,37} However, profound cardiovascular adaptations also include increased stroke volume, which increases wall tension and shear stress of the central artery, and consequently, may offset the vasodilatory effect on PWV.¹ The more profound increase in PWV in the postpartum PE group may indicate a failure of the peripheral and microvasculature adaptations in pregnancy to mitigate the impact that the increased cardiac output and stroke volume has on the aortic arch elasticity.

Limitations

The sample size of each cohort was limited. Of the 14 pregnant women, only four were in the third trimester, so we were unable to examine the potential for longitudinal changes between the second and third trimesters. Further, there were only nine postpartum women total, and from such a small dataset the results do not warrant a meaningful interpretation regarding the pathophysiology of preeclampsia.

Another potential limitation of this study is that pregnant women were examined at 1.5T and compared to nonpregnant controls examined at 3T field strength. MRI quantification based on MR signal can lead to systematic errors, even between two scanners with the same field strength and operating platform.³⁸ However, the proposed MRI protocol relies on the phase of the MRI signal to quantify the physiologic parameters (except for femoral artery FMD_L). In the latter case, the only requirement to be met is adequate signal contrast between lumen and vessel wall for estimation of the lumen area. The parameters extracted from dynamic oximetry, velocimetry, and aortic arch PWV all rely on signal phase and the primary source of phase error is static field inhomogeneity. The MRI principle of velocimetry and PWV are identical and the method is fundamentally robust against static field inhomogeneity because the phase difference is taken between two images acquired with the same echo time.³⁹ Dynamic oximetry is more susceptible to field inhomogeneity; however, the superficial femoral vein is a deep-lying vessel at mid-thigh and the primary effect of inhomogeneity caused by air-tissue interfaces is considerably mitigated and further reduced with retrospective correction.³¹ Thus, we are confident that the comparisons are valid despite the different field strengths. Nonetheless, it is indicated in future studies to minimize these potential confounders.

Conclusion

There remains much to learn about the complex vascular adaptations in pregnancy and preeclampsia.⁴ Our pilot study suggests that MRI has the potential to provide clinically useful information on systemic vascular function associated with maternal cardiovascular adaptations during pregnancy with greater detail.

REFERENCES

1. Sanghavi M, Rutherford JD. Cardiovascular physiology of pregnancy. *Circulation* 2014;130:1003-1008.
2. Tomimatsu T, Mimura K, Endo M, Kumasawa K, Kimura T. Pathophysiology of preeclampsia: An angiogenic imbalance and long-lasting systemic vascular dysfunction. *Hypertens Res* 2017;40:305-310.
3. Hutcheon JA, Lisonkova S, Joseph KS. Epidemiology of pre-eclampsia and the other hypertensive disorders of pregnancy. *Best Pract Res Clin Obstet Gynaecol* 2011;25:391-403.
4. Mosca L, Benjamin EJ, Berra K, et al. Effectiveness-based guidelines for the prevention of cardiovascular disease in women—2011 update: A guideline from the American Heart Association. *J Am Coll Cardiol* 2011;57:1404-1423.
5. Smith GN, Pudwell J, Walker M, Wen SW. Ten-year, thirty-year, and lifetime cardiovascular disease risk estimates following a pregnancy complicated by preeclampsia. *J Obstet Gynaecol Can* 2012;34: 830-835.
6. Celermajer DS, Sorensen KE, Gooch VM, et al. Non-invasive detection of endothelial dysfunction in children and adults at risk of atherosclerosis. *Lancet* 1992;340:1111-1115.
7. Philpott A, Anderson TJ. Reactive hyperemia and cardiovascular risk. *Arterioscler Thromb Vasc Biol* 2007;27:2065-2067.

8. Sorensen KE, Celermajer DS, Spiegelhalter DJ, et al. Non-invasive measurement of human endothelium dependent arterial responses: Accuracy and reproducibility. *Br Heart J* 1995;74:247-253.
9. Hardie KL, Kinlay S, Hardy DB, Wlodarczyk J, Silberberg JS, Fletcher PJ. Reproducibility of brachial ultrasonography and flow-mediated dilatation (FMD) for assessing endothelial function. *Aust N Z J Med* 1997;27:649-652.
10. Bots ML, Westerink J, Rabelink TJ, de Koning EJ. Assessment of flow-mediated vasodilatation (FMD) of the brachial artery: Effects of technical aspects of the FMD measurement on the FMD response. *Eur Heart J* 2005;26:363-368.
11. Sejda T, Pit'ha J, Svandova E, Poledne R. Limitations of non-invasive endothelial function assessment by brachial artery flow-mediated dilatation. *Clin Physiol Funct Imaging* 2005;25:58-61.
12. Potter K, Reed CJ, Green DJ, Hankey GJ, Arnolda LF. Ultrasound settings significantly alter arterial lumen and wall thickness measurements. *Cardiovasc Ultrasound* 2008;6:6.
13. Weissgerber TL, Milic NM, Milin-Lazovic JS, Garovic VD. Impaired flow-mediated dilation before, during, and after preeclampsia: A systematic review and meta-analysis. *Hypertension* 2016;67:415-423.
14. Lopes van Balen VA, van Gansewinkel TAG, de Haas S, et al. Physiological adaptation of endothelial function to pregnancy: Systematic review and meta-analysis. *Ultrasound Obstet Gynecol* 2017;50:697-708.
15. Kim JW, Park CG, Hong SJ, et al. Acute and chronic effects of cigarette smoking on arterial stiffness. *Blood Press* 2005;14:80-85.
16. Mitchell GF, Vita JA, Larson MG, et al. Cross-sectional relations of peripheral microvascular function, cardiovascular disease risk factors, and aortic stiffness: The Framingham Heart Study. *Circulation* 2005;112:3722-3728.
17. Safar ME, London GM, Plante GE. Arterial stiffness and kidney function. *Hypertension* 2004;43:163-168.
18. Willum-Hansen T, Staessen JA, Torp-Pedersen C, et al. Prognostic value of aortic pulse wave velocity as index of arterial stiffness in the general population. *Circulation* 2006;113:664-670.
19. Asmar R, Benetos A, Topouchian J, et al. Assessment of arterial distensibility by automatic pulse wave velocity measurement. Validation and clinical application studies. *Hypertension* 1995;26:485-490.
20. Laurent S, Cockcroft J, Van Bortel L, et al. Expert consensus document on arterial stiffness: Methodological issues and clinical applications. *Eur Heart J* 2006;27:2588-2605.
21. Van Bortel LM, Duprez D, Starmans-Kool MJ, et al. Clinical applications of arterial stiffness, Task Force III: Recommendations for user procedures. *Am J Hypertens* 2002;15:445-452.
22. Hausvater A, Giannone T, Sandoval YH, et al. The association between preeclampsia and arterial stiffness. *J Hypertens* 2012;30:17-33.
23. Estensen ME, Remme EW, Grindheim G, et al. Increased arterial stiffness in pre-eclamptic pregnancy at term and early and late postpartum: A combined echocardiographic and tonometric study. *Am J Hypertens* 2013;26:549-556.
24. Langham MC, Floyd TF, Mohler ER 3rd, Magland JF, Wehrli FW. Evaluation of cuff-induced ischemia in the lower extremity by magnetic resonance oximetry. *J Am Coll Cardiol* 2010;55:598-606.
25. Langham MC, Zhou Y, Chirico EN, et al. Effects of age and smoking on endothelial function assessed by quantitative cardiovascular magnetic resonance in the peripheral and central vasculature. *J Cardiovasc Magn Reson* 2015;17:19.
26. Caporale A, Langham MC, Guo W, Johncola A, Chatterjee S, Wehrli FW. Acute effects of electronic cigarette aerosol inhalation on vascular function detected at quantitative MRI. *Radiology* 2019;293:97-106.
27. ACOG Practice Bulletin No. 202: Gestational hypertension and preeclampsia. *Obstet Gynecol* 2019;133:e1-e25.
28. Langham MC, Magland JF, Epstein CL, Floyd TF, Wehrli FW. Accuracy and precision of MR blood oximetry based on the long paramagnetic cylinder approximation of large vessels. *Magn Reson Med* 2009;62:333-340.
29. Langham MC, Jain V, Magland JF, Wehrli FW. Time-resolved absolute velocity quantification with projections. *Magn Reson Med* 2010;64:1599-1606.
30. Langham MC, Li C, Magland JF, Wehrli FW. Nontriggered MRI quantification of aortic pulse-wave velocity. *Magn Reson Med* 2011;65:750-755.
31. Langham MC, Magland JF, Floyd TF, Wehrli FW. Retrospective correction for induced magnetic field inhomogeneity in measurements of large-vessel hemoglobin oxygen saturation by MR susceptometry. *Magn Reson Med* 2009;61:626-633.
32. Kapur JN, Sahoo PK, Wong ACK. A new method for gray-level picture thresholding using entropy of the histogram. *Comput Vis Graph Image Process* 1985;29:273-285.
33. Langham M, Wehrli F. Simultaneous mapping of temporally-resolved blood flow velocity and oxygenation in femoral artery and vein during reactive hyperemia. *J Cardiovasc Magn Reson* 2011;13:66.
34. Macedo ML, Luminoso D, Sawidou MD, McEniery CM, Nicolaides KH. Maternal wave reflections and arterial stiffness in normal pregnancy as assessed by applanation tonometry. *Hypertension* 2008;51:1047-1051.
35. Mannaerts D, Faes E, Cornette J, et al. Low-flow mediated constriction as a marker of endothelial function in healthy pregnancy and preeclampsia: A pilot study. *Pregnancy Hypertens* 2019;17:75-81.
36. Wilenius M, Tikkakoski AJ, Tahvanainen AM, et al. Central wave reflection is associated with peripheral arterial resistance in addition to arterial stiffness in subjects without antihypertensive medication. *BMC Cardiovasc Disord* 2016;16:131.
37. Poppas A, Shroff SG, Korcarz CE, et al. Serial assessment of the cardiovascular system in normal pregnancy. Role of arterial compliance and pulsatile arterial load. *Circulation* 1997;95:2407-2415.
38. Stikov N, Boudreau M, Levesque IR, Tardif CL, Barral JK, Pike GB. On the accuracy of T1 mapping: Searching for common ground. *Magn Reson Med* 2015;73:514-522.
39. Wymer DT, Patel KP, Burke WF 3rd, Bhatia VK. Phase-contrast MRI: Physics, techniques, and clinical applications. *Radiographics* 2020;40:122-140.